The New Vector Fitting Approach to Modeling of UWB Channels Containing Convex Obstacles

Piotr Górniak
Department of Electronics and Telecommunication
Poznan University of Technology
Poznan, Poland
pgorniak@et.put.poznan.pl

Wojciech Bandurski
Department of Electronics and Telecommunication
Poznan University of Technology
Poznań, Poland
wojciech.bandurski@put.poznan.pl

Abstract— **The paper presents the new approach to time-domain modelling of UWB containing convex obstacles. It uses vector fitting algorithm for deriving the closed form impulse response of the convex obstacle, which can be modelled by conducting convex objects (e.g. cylinders). Vector fitting algorithm uses an appropriate argument of approximation in order to obtain the closed form impulse response. The correctness and accuracy of the model is verified by simulations of an Ultra Wide Band (UWB) impulse distortion.**

Keywords- UWB; UTD; time-domain; impulse response; vector fitting.

I. INTRODUCTION

The paper describes time-domain modeling of UWB channels containing obstacles which can be modelled by very good conducting convex objects. We consider theoretical type of channel modelling incorporating ray tracing algorithms. Among the examples of obstacles, which may occur in the channel and can be modelled by convex models (e.g. cylinders), are round pillars in buildings and especially people, whose existence in a shorter range channel have to be taken into account [2]. The goal of this paper is to present the closed form impulse response of the diffraction ray, referring to a specific path of an UWB impulse "echo". This problem was considered in [1], [3]. The main disadvantage of the solutions given in [1] and [3] is that they give two separate formulas for two specific cases. The first of them relates to the transmission problem of baseband UWB pulse propagation or transmission problem of modulated (carrier) UWB pulse with smaller values of the object radius. The second of them concerns the transmission problem of modulated (carrier) UWB pulse with more general values of the cylinder radius or the radar issues when the wave creeps the obstacle on longer distances (arc lengths). In this paper we present the way of obtaining the general case closed form impulse response of a conducting separate convex object (2D cylinder). The procedure incorporates vector fitting algorithm [4] with appropriate determination of an approximation argument. The approximation argument is derived in the way that it includes frequency and almost all the necessary parameters of the convex object. With the usage of the introduced procedure we derive the closed form impulse response of the separate conducting convex object (2D cylinder, arc) placed between given positions of transmitting and receiving antennas for the case of obstacles with smaller radius values (e.g. case of human beings). This limitation is done in order to decrease the number of the desired impulse response components. The procedure given in this article can be successfully applied also to more general case. Then we must increase the domain of approximation which results in bigger number of poles that should be considered in vector fitting algorithm.

The derived procedure and closed form impulse response are verified by the simulations results where the results obtained with the usage of the new impulse response are compared with the IFFT results.

The paper is organized as follows. In Section 2 of the paper it is shown the model of the separate convex obstacle. The introduced procedure and new closed form impulse response of conducting convex object is given in Section 3. In Section 4 we present the simulations results. Finally in Section 5 we conclude the paper.

II. MODEL OF A CONVEX OBSTACLE

The exact UTD expression for a frequency-domain diffraction coefficient for one convex obstacle 2D model (arc) has the form presented in (1) [3], and the parameters of the model are indicated in Fig. 1, [5].

$$H_A(\omega) = -m\sqrt{\frac{2}{\beta}}e^{-j\frac{\pi}{4}}\left(\frac{-F(X_d))}{2\xi_d\sqrt{\pi}} + \begin{Bmatrix} p^*(\xi_d) \\ q^*(\xi_d) \end{Bmatrix}\right) \quad (1)$$

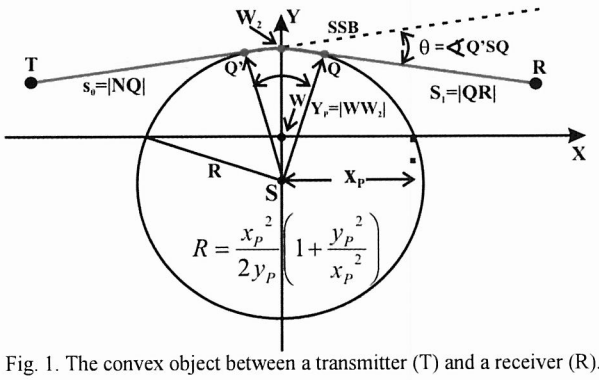

Fig. 1. The convex object between a transmitter (T) and a receiver (R).

The diffraction coefficient (transfer function $H_A(\omega)$) in (1) does not include the delay terms and spreading factor. The parameters used in (1) are described by (2a), (2b) and (2c) [5],

$$m(\omega,R)=\left(\frac{\omega\cdot R}{2\cdot v}\right)^{1/3}, \tag{2a}$$

$$\xi_d(\omega,\theta,R)=m(\omega,R)\cdot\theta, \tag{2b}$$

$$X_d=\frac{\omega L\theta^2}{2v}, \tag{2c}$$

where $\beta=\omega/v$, v is the speed of electromagnetic wave propagation and L, given by (3) [5], is the distance coefficient ensuring the fields values continuity along the shadow boundary SSB, $F(X_d)$ is the transition function and $p^*(x)$ and $q^*(x)$ are the special Fock scattering functions for the case of soft and hard polarization respectively [5].

$$L=\frac{|TQ'||QR|}{|TQ'|+|QR|} \tag{3}$$

Before we will give the procedure for deriving the new impulse response we will first remind the results presented in [1] and [3]. Frequency response (1) can be decomposed into two components:

$$H_1(\omega)=m\sqrt{\frac{2}{\beta}}e^{-j\frac{\pi}{4}}\frac{F(X_d)}{2\xi_d\sqrt{\pi}} \tag{4a}$$

$$H_2(\omega)=-m\sqrt{\frac{2}{\beta}}e^{-j\frac{\pi}{4}}p^*(\xi_d) \tag{4b}$$

Each of the above components can be transformed into the time-domain separately. The equivalent of (4a) in time-domain is give by:

$$h_1(t)=\frac{L\cdot\theta}{2\pi\sqrt{v\cdot t}\left(t+\frac{X}{v}\right)} \tag{5a}$$

where:

$$X=\frac{L\theta^2}{2}. \tag{5b}$$

The corresponding results taken from [1] and [3] concerning the second component of $H_A(\omega)$ are given for two separate cases, introduced in section 1 of the paper. The first of them are applicable when for all considered frequencies of UWB incident pulse and the parameters of the scenario $\xi_d \le \xi_{dTh}$ [1] which yields the following condition:

$$\left(\frac{\pi\cdot f\cdot R}{v}\right)^{\frac{1}{3}}\cdot\theta\le\xi_{dTh} \tag{6}$$

The second of them is a complementary case, $\xi_d > \xi_{dTh}$. The aim of the considerations which follow is to obtain one formula for the time-domain equivalent of (4b), which will be applicable to more general case including transmission as well as radar (sensor) problems.

III. THE NEW IMPULSE RESPONSE OF A CONVEX OBSTACLE

The general impulse response for all considered domain of ξ_d is derived in the following way. First $H_2(\omega)$ is rearranged to the form of (7a-c) which is the product of two factors (functions). The first of them is independent of the frequency, is a constant real function (from a frequency point of view). The second factor is a function of a new variable ξ_{sub} (8). This new variable contributes all frequency as well as convex object parameters. This decomposition of $H_2(\omega)$ allows the derivation of the general approximation of $H_2(\omega)$ by using vector fitting algorithm. According to (2a) and (2b) the new variable is equal to (9). The form of this new variable was not only chosen for the reason of gathering all the frequency contributions but also for other very important reasons. The second reason is the observation that an attenuated Fock scattering functions are best fitted with this form of the new variable. The third, not less important reason for choosing such form of this variable, is that it allows in consequence easy transformation of the approximating vector fitting Laplace transform to the time-domain.

$$H_2(\xi_{sub})=H_{21}(R)\cdot H_{22}(\xi_{sub}) \tag{7a}$$

$$H_{21}(R)=\sqrt{R\cdot\theta} \tag{7b}$$

$$H_{22}(\xi_{sub})=e^{-j\pi/4}\frac{\left\{\begin{matrix}p^*\left(\xi_{sub}^{1/3}\right)\\ q^*\left(\xi_{sub}^{1/3}\right)\end{matrix}\right.}{\xi_{sub}^{1/6}} \tag{7c}$$

$$\xi_{sub}=(\xi_d)^3 \tag{8}$$

$$\xi_{sub}=\frac{\omega\cdot R}{2\cdot v}\theta^3 \tag{9}$$

With the usage of the vector fitting algorithm we obtain the approximation of $H_{22}(\xi_{sub})$ with the variable $p=j\xi_{sub}$. The number of necessary poles, which should be used, depends on the established limits of the approximation domain. For all considered domain the approximation deviation must be low enough (for example 0.1%). We can set for example the value of lower limit of the approximation domain to 10^{-12} which is smaller than the value of (9) for the case of R=0.25m, lower frequency of the transmitted UWB pulse f_L=0.5 GHz and creeping arc length θ=0,01°. The mentioned radius value relates to those used in the literature to model the human body presence and theta angle value is almost the grazing incidence case. The assumption of such value of this angle for the grazing incidence case does not cause meaningful error in UWB pulse propagation analysis. Then we can set the upper

limit of the approximation domain to 10^4, which is bigger from the value of (9) for the case of R=0.50m, upper frequency of the transmitted UWB pulse f_H=10GHz and θ=270°. This case may be related to radar (sensor) problems when the wave creeps the obstacle on a longer arc length. When these limits of approximation domain are set, vector fitting algorithm creates very good quality of approximation when 25 poles are used. Better results of approximation are obtained when log scale sampling is used instead of linear. Vector fitting algorithm gives the approximating equivalent of $H_{22}(\xi_{sub})$ in the form (N=25 for the described approximation domain):

$$H_{22}(j\xi_{sub},N)\approx\left[D+E\cdot j\xi_{sub}+\sum_{n=1}^{N}\frac{C_n}{j\xi_{sub}-A_n}\right] \tag{10}$$

When we substitute (9) to (10) and (10) to (7a) we obtain the Laplace transform equivalent of $H_2(\omega)$ in the following formulas (s=jω):

$$H_2(j\omega,N)\approx\sqrt{R\cdot\theta}\left[D+j\omega\cdot\frac{E\cdot R\cdot\theta^3}{2\cdot v}+\sum_{n=1}^{N}\frac{C_n}{j\omega\cdot\frac{R\cdot\theta^3}{2\cdot v}-A_n}\right] \tag{11a}$$

$$H_2(s,N)\approx\sqrt{R\cdot\theta}\left[D+s\cdot\frac{E\cdot R\cdot\theta^3}{2\cdot v}+\sum_{n=1}^{N}\frac{C_n\cdot 2v/(R\cdot\theta^3)}{s-A_n\cdot 2v/(R\cdot\theta^3)}\right] \tag{11b}$$

Finally using the inverse Laplace transform for (11b) and having (5a) we can give the formula for the new impulse response of a convex conducting obstacle applicable for transmission as well as radar (sensor) problems:

$$h(t,N)\approx\frac{L\cdot\theta}{2\pi\sqrt{v\cdot t}\left(t+\frac{X}{v}\right)}+\ldots \tag{12}$$

$$\sqrt{R\cdot\theta}\left[\delta(t)\cdot D+\delta'(t)\cdot\frac{E\cdot R\cdot\theta^3}{2\cdot v}+\sum_{n=1}^{N}\frac{C_n\cdot 2v}{R\cdot\theta^3}\cdot e^{-A_n\cdot 2v\cdot t/(R\cdot\theta^3)}\right]$$

IV. NUMERICAL SIMULATIONS

In this section we examine the accuracy of the derived new impulse response. In order to do this we calculate the distortion of an UWB pulse caused by conducting convex object. We examined the baseband UWB pulse (13a) and the mid-band UWB pulse (13b) distortion.

$$w_1(t,t_c,a)=\left[1-4\pi\left(\frac{t-t_c}{a}\right)^2\right]e^{-2\pi\left(\frac{t-t_c}{a}\right)^2} \tag{13a}$$

$$w_2(t,f_c,k)=\left(\frac{8\cdot k}{\pi}\right)^{\frac{1}{4}}\frac{1}{\sqrt{1+e^{\frac{2\pi^2 f_c^2}{k}}}}e^{-k\cdot t^2}\cos(2\pi\cdot f_c\cdot t) \tag{13b}$$

The results obtained with the usage of the new impulse response are compared with the results incorporating IFFT. The results of the distorted UWB pulse do not include the effects of an attenuation of the signal in the air and the delay indicated by the factor δ(t-s/v) in an impulse response, where s is the total length of air distances and creeping distances that propagates UWB pulse along the creeping ray. The results are presented in Fig. 2a to Fig. 2d. The figures present the shapes of the distorted and incident UWB pulses. The amplitudes of the pulses are normalized to the amplitude of the distorted pulse. The time domain axis is scaled in ns.

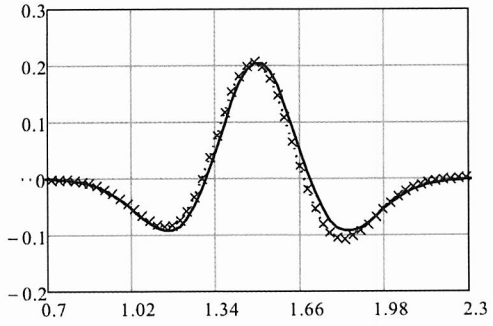

Fig. 2a. The shapes of the distorted baseband UWB pulses caused by a convex obstacle with the scenario parameters a=0.7 ns and t_c=1.5ns, R=0,25m, θ=0.01, calculated with the usage of the derived impulse response (dot line) and by IFFT (cross line) compared to the shape of the incident pulse (solid line) for soft polarization case.

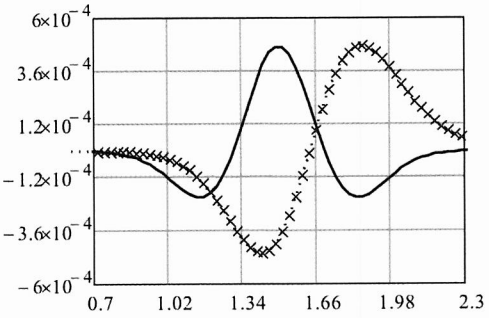

Fig. 2b. The shapes of the distorted baseband UWB pulses caused by a convex obstacle with the scenario parameters a=0.7 ns and t_c=1.5ns, R =0,25m, θ=π, calculated with the usage of the derived impulse response (dot line) and by IFFT (cross line) compared to the shape of the incident pulse (solid line) for hard polarization case.

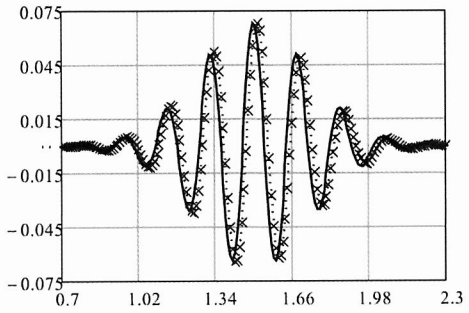

Fig. 2c. The shapes of the distorted mid-band UWB pulses caused by a convex obstacle with the scenario parameters t_c=1.5ns, t_c=1.5ns, f_c=5.5GHz, $k=3\cdot10^3$, R= 0,25m, θ=0.2, calculated with the usage of the derived impulse response (dot line) and by IFFT (cross line) compared to the shape of the incident pulse (solid line) for soft polarization case.

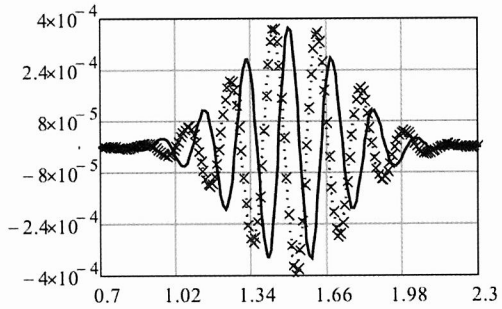

Fig. 2d. The shapes of the distorted mid-band UWB pulses caused by a convex obstacle with the parameters t_c=1.5ns, t_c=1.5ns, f_c=5.5GHz, $k=3\cdot10^3$, R= 0,25m, $\theta=\pi$, calculated with the usage of the derived impulse response (dot line) and by IFFT (cross line) compared to the shape of the incident pulse (solid line) for hard polarization case.

V. CONCLUSIONS

We presented in the paper the procedure for obtaining the closed form general case impulse response of the creeping ray on a conducting convex obstacle. The new impulse response can be applied to transmission as well as radar (sensor) problems. The derived new impulse response was positively verified by the fact of very good agreement between the time domain calculation results with the IFFT results. Further research should concern the general case impulse response for dielectric convex objects and the cascade of convex objects.

REFERENCES

[1] P. Górniak, W. Bandurski, „ Time Domain Transition Zone Diffraction on Convex Obstacles", "Ultra-Wideband, Short-Pulse Electromagnetics 9", Springer Verlag, April 2010

[2] Kashiwagi, T. Imai, "Time-varying Path-shadowing Model for Indooe Populated Environments " . IEEE Transactions on Vehicular Technology, vol. 59, no. 1, pp. 16–29, January. 2010

[3] P. Górniak, W. Bandurski "Direct Time Domain Analysis of an UWB Pulse Distortion by Convex Objects with the Slope Diffraction Included", IEEE Transactions on Antennas and Propagation., vol. 56, no. 9, September 2008, pp. 3036–3044.

[4] B. Gustavsen, A. Semlyen, "Rational approximation of frequency domain response by vector fitting", IEEE Tran. on Power Delivery, vol.14, no. 3, 1999, pp. 1052-1061.

[5] D. A. McNamara, Introduction to the uniform geometrical theory of diffraction, Artech House, Boston, London, 1990.